Chapter 4

Peristaltic transport of a conducting fluid in a vertical asymmetric channel

4.1 Introduction

Most of the contributions in the study of peristaltic transport deal with the peristaltic flow in symmetric channels. Although a wide range of understanding about peristaltic pumping is possible by considering a channel to be a symmetric one, there are some physiological systems such as uterus in which asymmetry plays an important role in transporting the uterine (Eytan and Elad 1999). Mekheimer (2003) studied non-linear peristaltic transport through a porous medium in an inclined channel considering the effect of gravity. The first experimental work on peristalsis is reported by Latham (1966). Later Weinberg et al. (1971) confirmed through experiments the use of Lagrangian approach for discussing peristaltic pumping.

Jaffrin and shaprio (1971) applied wave frame analysis and discussed pumping characteristics, trapping and reflux which are important in peristaltic transport. A thesis on peristaltic transport in a channel with flexible porous walls contained within the channel with fixed walls has been presented by Rees (1988) and it contains the review of literature up to 1988. Srivastava and Srivastava

(1995) have studied the effects of Poiseuille flow on peristaltic transport of a particulate suspension.

The importance of yield stress effects on peristaltic pumping is studied by vajravelu et al. (2005a, 2005b). They have considered the bio fluid to be Herschel Bulkley fluid and deduced the trapping limits for power law and Bingham fluids. In order to have a better understanding the intra-uterine fluid motion in a non-pregnant uterus Mishra and Ramachandra Rao (2003) studied the flow in an asymmetric channel generated by peristaltic waves propagating on the walls. The inertia and curvature effects on the peristaltic flow of a Newtonian fluid in an asymmetric channel are investigated by Mishra (2004) using perturbation technique.

Xiao and Damodaran (2002) have investigated numerically the peristaltic pumping in axisymmetric tubes. Pozrikidis (1987) has studied the peristaltic flow under Stokes approximation by a boundary integral method. Selverov and stone (2001) and Yi et al. (2002) have discussed the peristaltic flows in two – dimensional channels using perturbation method to model micro electro mechanical systems in which fluid motion produces mixing without internal movement of the mechanical components.

In this chapter MHD peristaltic flow of an incompressible viscous fluid in a vertical asymmetric channel is investigated under long wavelength and low Reynolds number assumptions. The expressions for velocity distribution, the stream function, the volume flow rate and the pressure rise are obtained. The

effects of phase shift and Hartmann number on the pumping characteristics are discussed.

Mathematical formulation and Solution

We consider the peristaltic transport of a conducting viscous fluid in a vertical asymmetric channel with flexible walls with asymmetry being generated by the propagation of waves on the channel walls travelling with same speed c but with different amplitudes and phases. We assume that a uniform magnetic field strength B_0 is applied in the transverse direction to the direction of the flow (i. e., along the direction of the y-axis) and the induced magnetic field is assumed to be negligible. Fig 4.1. shows the physical model of the asymmetric channel.

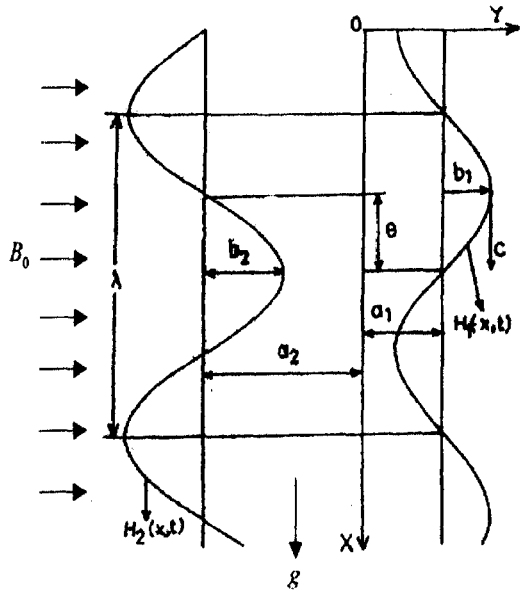

Fig 4.1. Physical Model

The channel walls are given by

$$Y = H_1(X,t) = a_1 + b_1 \cos\frac{2\pi}{\lambda}(X - ct) \qquad \text{(upper wall)} \quad (4.1a)$$

$$Y = H_2(X,t) = -a_2 - b_2 \cos\left(\frac{2\pi}{\lambda}(X - ct) + \theta\right) \quad \text{(lower wall)} \quad (4.1b)$$

where b_1, b_2 are amplitudes of the waves, λ is the wavelength, $a_1 + a_2$ is the width of the channel, θ is the phase difference ($0 \le \theta \le \pi$) and t is the time.

We introduce a wave frame of reference (x, y) moving with velocity c in which the motion becomes independent of-time when the channel length is an integral multiple of the wavelength and the pressure difference at the ends of the channel is a constant (Shapiro et al. 1969). The transformation from the fixed frame of reference (X, Y) to the wave frame of reference (x, y) is given by

$$x = X - c\,t,\ y = Y,\ u = U - c,\ v = V \quad \text{and} \quad p(x) = P(X, t),$$

where (u, v) and (U, V) are the velocity components, p and P are pressures in the wave and fixed frames of reference, respectively.

The equations governing the flow in wave frame of reference are given by

$$\frac{\partial u}{\partial x} + \frac{\partial v}{\partial y} = 0, \qquad (4.2)$$

$$u\frac{\partial u}{\partial x} + v\frac{\partial u}{\partial y} = -\frac{1}{\rho}\frac{\partial p}{\partial x} + \frac{\mu}{\rho}\left(\frac{\partial^2 u}{\partial x^2} + \frac{\partial^2 u}{\partial y^2}\right) - \frac{\sigma_e B_0^2}{\rho}u + g, \qquad (4.3)$$

$$u\frac{\partial v}{\partial x} + v\frac{\partial v}{\partial y} = -\frac{1}{\rho}\frac{\partial p}{\partial y} + \frac{\mu}{\rho}\left(\frac{\partial^2 v}{\partial x^2} + \frac{\partial^2 v}{\partial y^2}\right). \qquad (4.4)$$

where σ_e is the electrical conductivity of the fluid, ρ is the density, μ is the viscosity of the fluid and g is the acceleration due to gravity.

Introducing the following non-dimensional variables

$$\bar{x} = \frac{x}{\lambda}, \bar{y} = \frac{y}{a_1}, \bar{u} = \frac{u}{c}, \bar{v} = \frac{v}{c\delta}, \delta = \frac{a_1}{\lambda}, d = \frac{a_2}{a_1}$$

$$\bar{p} = \frac{pa_1^2}{\mu c\lambda}, h_1 = \frac{H_1}{a_1}, h_2 = \frac{H_2}{a_1}, \phi_1 = \frac{b_1}{a_1}, \phi_2 = \frac{b_2}{a_1}.$$

in the governing equations (4.1-4.4), and dropping the bars, we get

$$h_1 = 1 + \phi_1 \cos 2\pi x,\ h_2 = -d - \phi_2 \cos(2\pi x + \theta) \tag{4.5}$$

$$\frac{\partial u}{\partial x} + \frac{\partial v}{\partial y} = 0, \tag{4.6}$$

$$\mathrm{Re}\,\delta\left(u\frac{\partial u}{\partial x} + v\frac{\partial u}{\partial y}\right) = -\frac{\partial p}{\partial x} + \left(\delta^2\frac{\partial^2 u}{\partial x^2} + \frac{\partial^2 u}{\partial y^2}\right) - M^2 u + \eta, \tag{4.7}$$

$$\mathrm{Re}\,\delta^3\left(u\frac{\partial v}{\partial x} + v\frac{\partial v}{\partial y}\right) = -\frac{\partial p}{\partial y} + \delta^2\left(\delta^2\frac{\partial^2 v}{\partial x^2} + \frac{\partial^2 v}{\partial y^2}\right). \tag{4.8}$$

where $\mathrm{Re} = \frac{\rho a_1 c}{\mu}$ is the Reynolds number, $\eta = \frac{a_1^2 g}{\nu c}$ is the gravity parameter, $M = B_0 a_1\sqrt{\frac{\sigma_e}{\mu}}$ is the Hartmann number and $\nu = \frac{\mu}{\rho}$ is the kinematic viscosity of the fluid.

Using long wavelength (i.e., $\delta << 1$) and negligible inertia (i.e., $\mathrm{Re} \to 0$) approximations, we have

$$\frac{\partial p}{\partial y} = 0, \qquad \frac{\partial^2 u}{\partial y^2} - M^2 u = P. \tag{4.9}$$

where $P = \frac{dp}{dx} - \eta$.

The corresponding non-dimensional boundary conditions are given as

$$u = -1 \qquad \text{at} \qquad y = h_1 \text{ and } y = h_2 \tag{4.10}$$

Solving equation (4.9) using the boundary conditions (4.10), we get

$$u = c_1 \cosh My + c_2 \sinh My - P/M^2 \tag{4.11}$$

where $c_1 = \dfrac{\left(-1 + P/M^2\right)\left[\sinh Mh_2 - \sinh Mh_1\right]}{\left[\cosh Mh_1 \sinh Mh_2 - \cosh Mh_2 \sinh Mh_1\right]}$ and

$$c_2 = \frac{\left(-1 + P/M^2\right)\left[\cosh Mh_1 - \cosh Mh_2\right]}{\left[\cosh Mh_1 \sinh Mh_2 - \cosh Mh_2 \sinh Mh_1\right]}$$

The volume flow rate in the wave frame is given as

$$q = \int_{h_2}^{h_1} u\,dy$$

$$= \frac{c_1}{M}\left(\sinh Mh_1 - \sinh Mh_2\right) + \frac{c_2}{M}\left(\cosh Mh_1 - \cosh Mh_2\right) - \frac{P}{M^2}\left(h_1 - h_2\right). \tag{4.12}$$

From (4.12), we have

$$P = \frac{dp}{dx} = \frac{qM^3 D_1 + D_2 M^2}{D_2 - (h_1 - h_2) M D_1} + \eta \tag{4.13}$$

where

$$D_1 = \cosh Mh_1 \sinh Mh_2 - \cosh Mh_2 \sinh Mh_1 \quad \text{and}$$

$$D_2 = (\cosh Mh_1 - \cosh Mh_2)^2 - (\sinh Mh_1 - \sinh Mh_2)^2$$

The instantaneous flux at any axial station is given by

$$Q(x,t) = \int_{h_2}^{h_1} (u+1)dy = q + h_1 - h_2 \tag{4.14}$$

The average volume flow rate over one wave period ($T = \lambda / c$) of the peristaltic wave is defined as

$$\bar{Q} = \frac{1}{T}\int_0^T Q dt = \frac{1}{T}\int_0^T (q + h_1 - h_2)dt = q + 1 + d. \tag{4.15}$$

The pressure rise over one wave length of the peristaltic wave is given by

$$\Delta p = \int_0^1 \frac{dp}{dx} dx = \int_0^1 \left[\frac{qM^3 D_1 + D_2 M^2}{D_2 - (h_1 - h_2) M D_1} + \eta \right] dx$$

$$= \int_0^1 \left[\frac{(\bar{Q} - 1 - d) M^3 D_1 + D_2 M^2}{D_2 - (h_1 - h_2) M D_1} + \eta \right] = \bar{Q} I_1 + I_2 + \eta. \tag{4.16}$$

where $I_1 = \int_0^1 \frac{M^3 D_1}{D_2 - (h_1 - h_2) M D_1} dx$ and $I_2 = \int_0^1 \frac{-(1+d) M^3 D_1 + D_2 M^2}{D_2 - (h_1 - h_2) M D_1} dx$.

The equation (4.16) can be rewritten as

$$\bar{Q} = \frac{\Delta p - I_2 - \eta}{I_1}. \tag{4.17}$$

4.3 Discussion of the Results

From Equation (4.11) we have evaluated the variation of axial velocity u as a function of y at $x=0.25$ for different values of M with $\phi_1=0.7$, $\phi_2=1.2$, $d=2$, $\eta=0.3$ and phase shift $\theta=0$ for (i) $\frac{dp}{dx}=-0.5$ b (ii) $\frac{dp}{dx}=0$ and (iii) $\frac{dp}{dx}=0.5$, and is shown in Fig 4.2. As M increases the maximum velocity increases for $\frac{dp}{dx}=-0.5$, $\frac{dp}{dx}=0$ and $\frac{dp}{dx}=0.5$. Further for non conducting fluid (i.e., $M=0$) the flow reverses.

The variation of axial velocity u with y for different values of M at $x=0.25$ with $\phi_1=0.7, \phi_2=1.2, d=2, \eta=0.3$ and $x=0.25$ with $\phi_1=0.7, \phi_2=1.2, d=2, \eta=0.3$ and $\theta=\frac{\pi}{4}$ for (i) $\frac{dp}{dx}=-0.5$, (ii) $\frac{dp}{dx}=0$ (iii) $\frac{dp}{dx}=0.5$ as shown in Fig 4.3. The maximum velocity increases as M increases for $\frac{dp}{dx}=-0.5$ $\frac{dp}{dx}=0$ and $\frac{dp}{dx}=0.5$. Further, for $\frac{dp}{dx}=0.5$ the flow is reversed in the direction of wave propagation on the channel for $M=0$ as shown in Fig 4.3. The same behavior holds for $\theta=\frac{\pi}{2}$, as shown in Fig 4.4. Finally we conclude as phase shift increases the maximum velocity decrease (Fig 4.2 – 4.4). Further the maximum velocity is more when compared with that in the horizontal channel.

The variation of axial velocity u as a function of y at $x=0.25$ for different values of gravity parameter η with $\phi_1=0.7$, $\phi_2=1.2$, $d=2$, $\theta=\frac{\pi}{4}$ and $M=0.5$, for (i) $\frac{dp}{dx}=-0.5$, (ii) $\frac{dp}{dx}=0$ (iii) $\frac{dp}{dx}=0.5$ as shown in Fig 4.5. It is observed that the maximum velocity increases as η increases for all values of $\frac{dp}{dx}$.

Using equation (4.16) we have evaluated the variation of time averaged flux with Δp for different values of phase shift θ, with $\phi_1=0.7$, $\phi_2=1.2$, $d=2$, $\eta=1$ for (1) $M=0.5$ and (ii) $M=1$ as shown in Fig 4.6. It is deserved that free pumping$(\Delta p=0)$ and co pumping $(\Delta p<0)$ increases as θ increases, where as pumping $(\Delta p>0)$ increases as θ increases, for an appropriately chosen $\Delta p>0$. Further as M increases $\bar{Q}$ increases.

Fig 4.7 shows the variation of time averaged flow rate $\bar{Q}$ with Δp for different values of phase shift θ with $\phi_1=0.7, \phi_2=1.2, d=2, M=0.5$ and for (i) $\eta=0$, (ii) $\eta=1$ and (iii) $\eta=2$. It is observed that free pumping ($\Delta p=0$) and co-pumping ($\Delta p<0$) increase as θ increases for the cases $\eta=1$ and 2 and pumping decreases as θ increases. Further as η increases $\bar{Q}$ increases. Another interesting observation here is that for $\eta=0$ the pumping and free pumping decrease as phase shift increases. It is clear that from Fig. 4.7 as η increases the point of intersection of pumping curves will move from 4th quadrant to 1st quadrant.

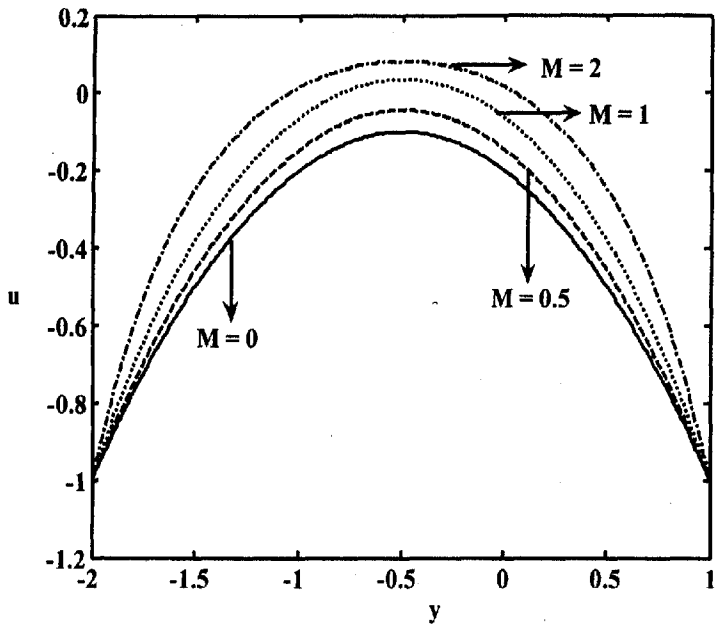

Fig 4.2(i). The variation of velocity u with y for different values of M with $\phi_1 = 0.7, \phi_2 = 1.2$, $d = 2, \eta = 0.3$, $x = 0.25$ and $\theta = 0$ for $\frac{dp}{dx} = -0.5$.

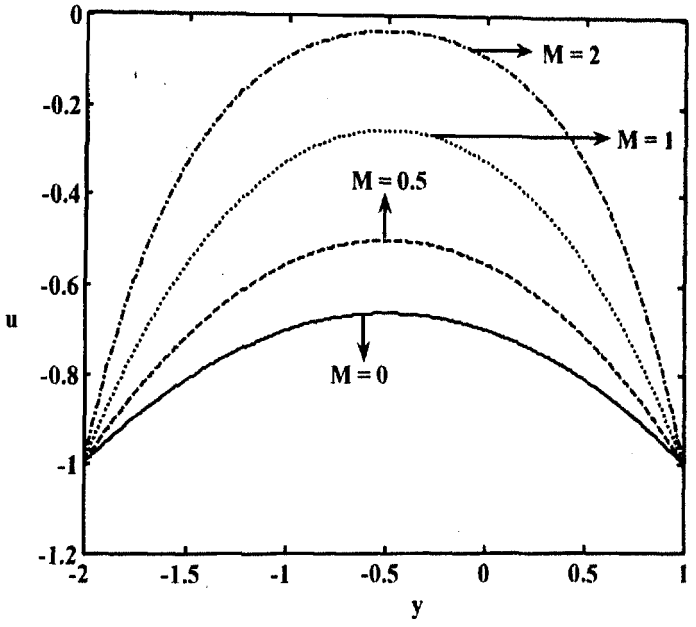

Fig 4.2(ii). The variation of velocity u with y for different values of M with $\phi_1 = 0.7, \phi_2 = 1.2$, $d = 2, \eta = 0.3$, $x = 0.25$ and $\theta = 0$ for $\frac{dp}{dx} = 0$.

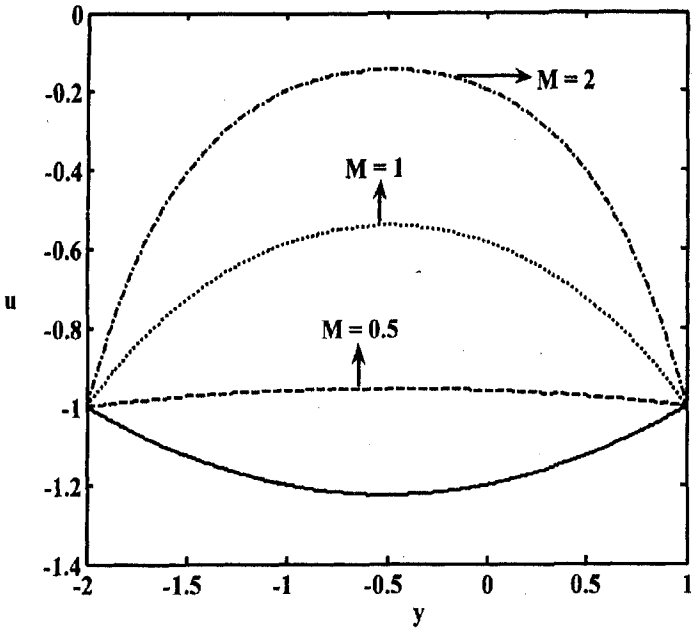

Fig 4.2(iii). The variation of velocity u with y for different values of M with $\phi_1 = 0.7, \phi_2 = 1.2$, $d = 2, \eta = 0.3$, $x = 0.25$ and $\theta = 0$ for $\frac{dp}{dx} = 0.5$.

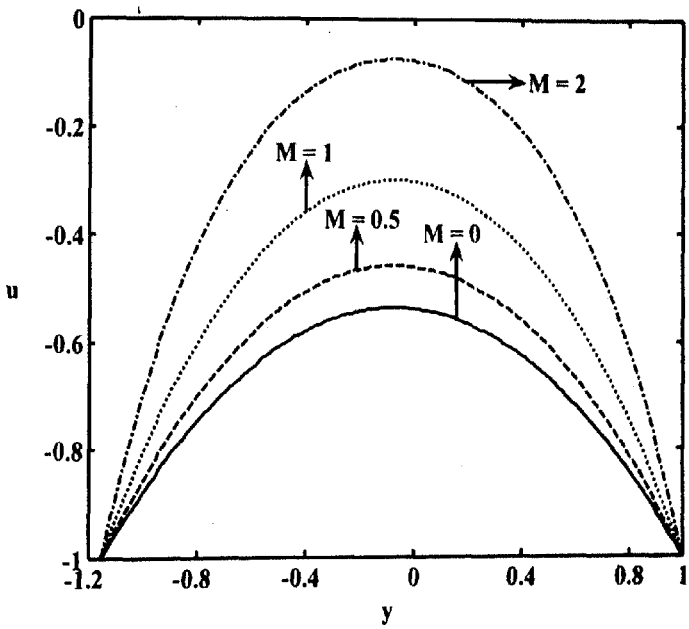

Fig 4.3(i). The variation of velocity u with y for different values of M with $\phi_1 = 0.7, \phi_2 = 1.2$, $d = 2, \eta = 0.3$, $x = 0.25$ and $\theta = \pi/4$ for $\frac{dp}{dx} = -0.5$.

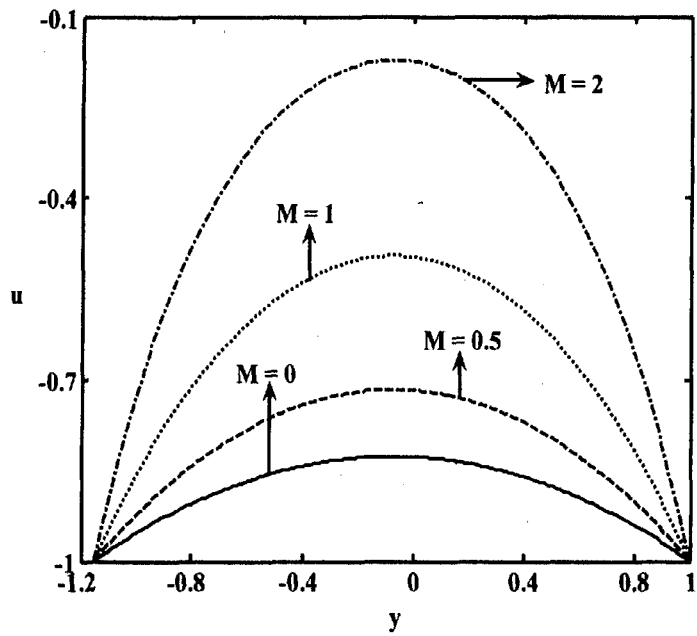

Fig 4.3(ii). The variation of velocity u with y for different values of M with $\phi_1 = 0.7, \phi_2 = 1.2$, $d = 2, \eta = 0.3$, $x = 0.25$ and $\theta = \pi/4$ for $\frac{dp}{dx} = 0$.

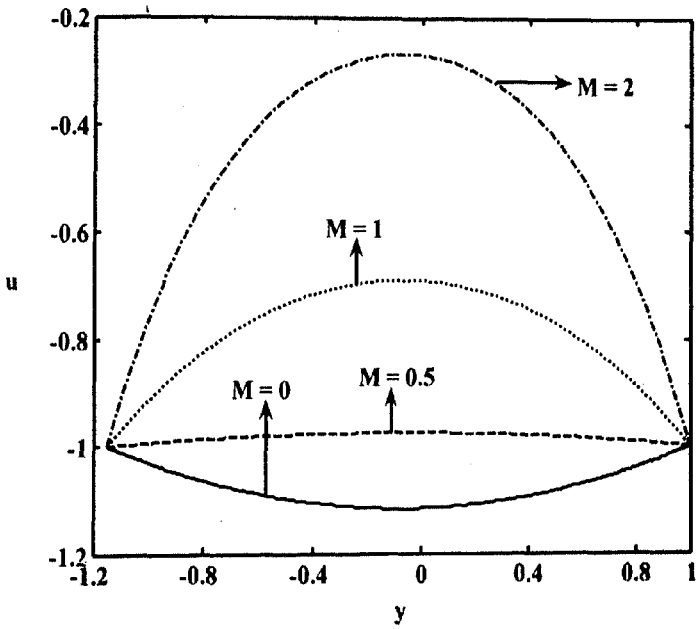

Fig 4.3(iii). The variation of velocity u with y for different values of M with $\phi_1 = 0.7, \phi_2 = 1.2$, $d = 2, \eta = 0.3$, $x = 0.25$ and $\theta = \pi/4$ for $\frac{dp}{dx} = 0.5$.

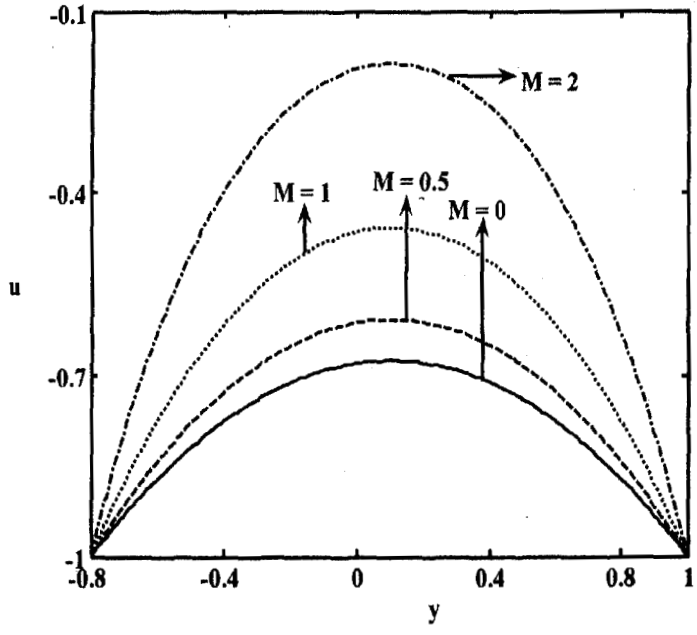

Fig 4.4(i). The variation of velocity u with y for different values of M with $\phi_1 = 0.7, \phi_2 = 1.2$, $d = 2, \eta = 0.3$, $x = 0.25$ and $\theta = \pi/2$ for $\frac{dp}{dx} = -0.5$.

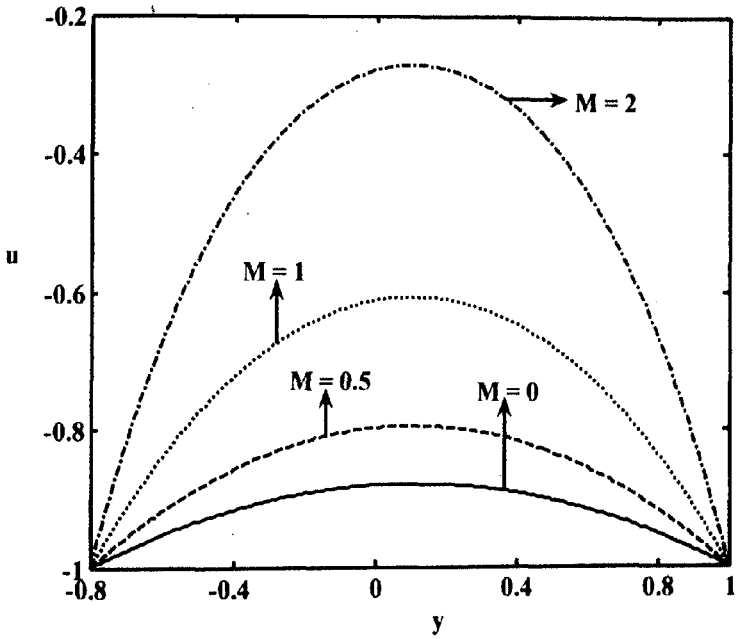

Fig 4.4(ii). The variation of velocity u with y for different values of M with $\phi_1 = 0.7, \phi_2 = 1.2$, $d = 2, \eta = 0.3$, $x = 0.25$ and $\theta = \pi/2$ for $\frac{dp}{dx} = 0$.

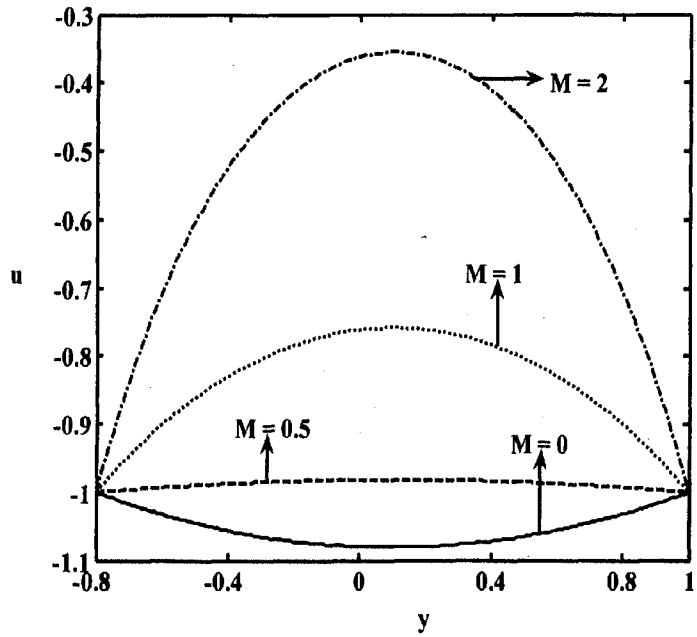

Fig 4.4(iii). The variation of velocity u with y for different values of M with $\phi_1 = 0.7, \phi_2 = 1.2$, $d = 2, \eta = 0.3$, $x = 0.25$ and $\theta = \pi/2$ for $\frac{dp}{dx} = 0.5$.

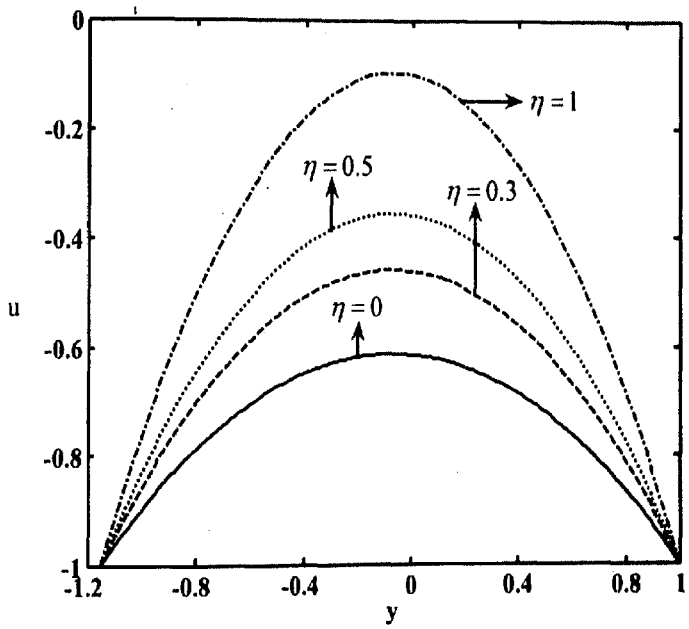

Fig 4.5(i). The variation of velocity u with y for different values of η with $\phi_1 = 0.7, \phi_2 = 1.2$, $d = 2, M = 0.5$, $x = 0.25$ and $\theta = \pi/4$ for $\frac{dp}{dx} = -0.5$.

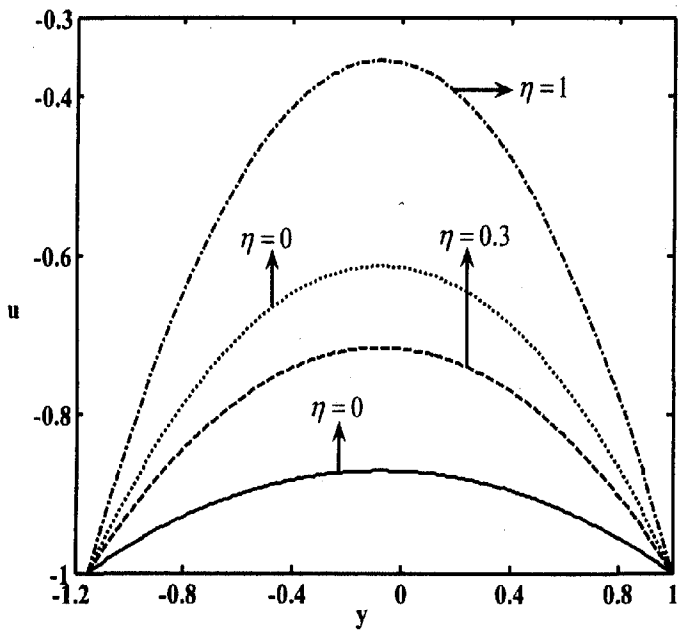

Fig 4.5(ii). The variation of velocity u with y for different values of η with $\phi_1 = 0.7, \phi_2 = 1.2$, $d = 2, M = 0.5$, $x = 0.25$ and $\theta = \pi/4$ for $\frac{dp}{dx} = 0$.

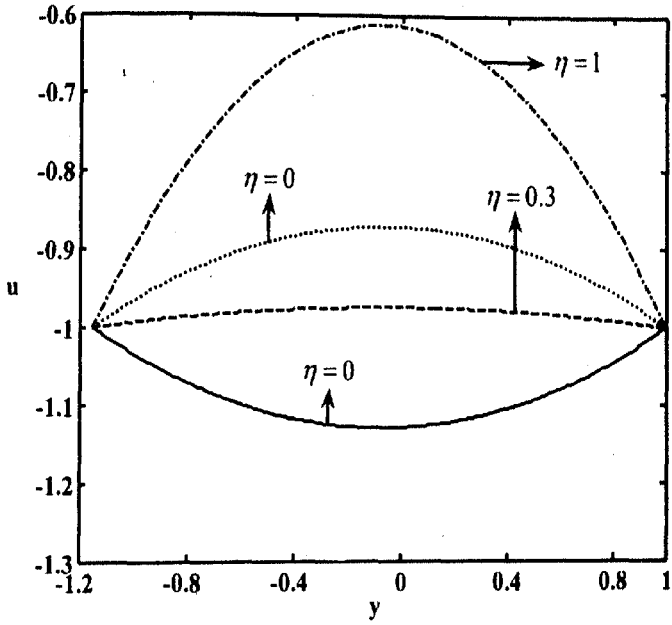

Fig 4.5(iii). The variation of velocity u with y for different values of η with $\phi_1 = 0.7, \phi_2 = 1.2$, $d = 2, M = 0.5$, $x = 0.25$ and $\theta = \pi/4$ for $\frac{dp}{dx} = 0.5$.

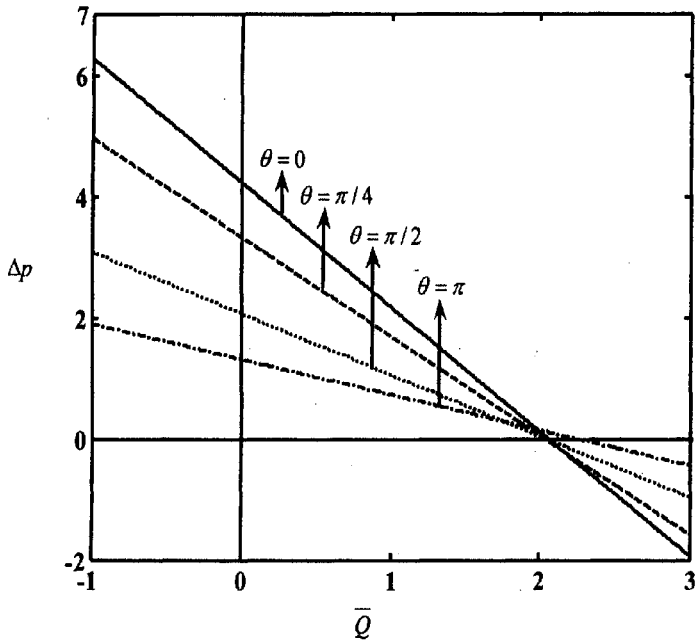

Fig 4.6(i). The variation of pressure rise Δp with time-averaged volume flow rate $\bar{Q}$ for different phase shifts with $d = 2, \phi_1 = 0.7, \phi_2 = 1.2$ and $\eta = 1$ for $M = 0.5$.

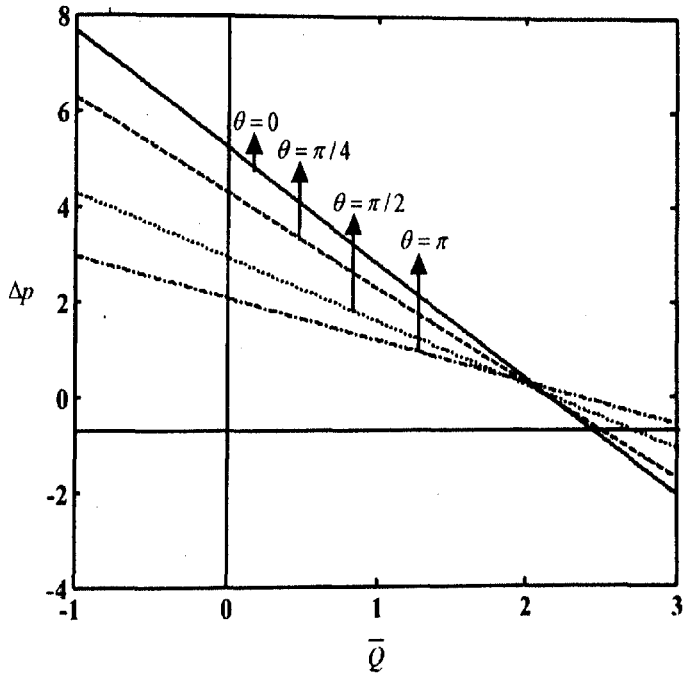

Fig 4.6(ii). The variation of pressure rise Δp with time-averaged volume flow rate $\bar{Q}$ for different phase shifts with $d = 2, \phi_1 = 0.7, \phi_2 = 1.2$ and $\eta = 1$ for (i) $M = 0.5$ and (ii) $M = 1$.

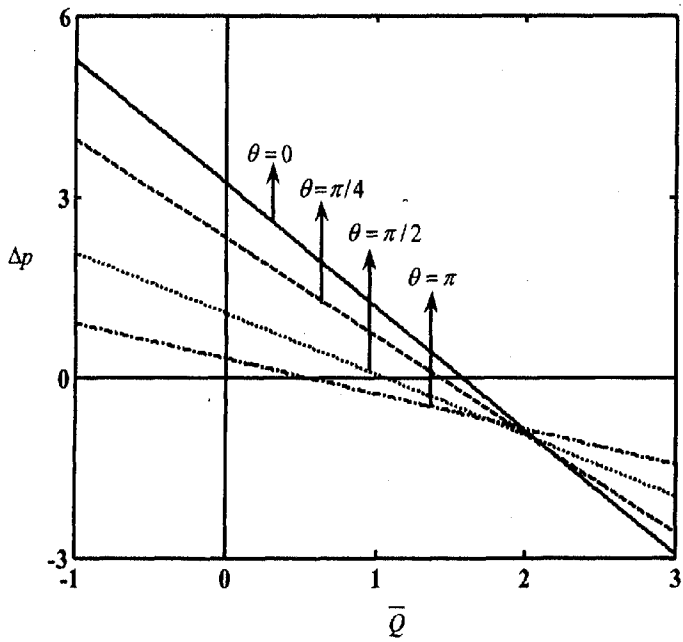

Fig 4.7(i). The variation of pressure rise Δp with time-averaged volume flow rate $\overline{Q}$ for different phase shifts with $d = 2, \phi_1 = 0.7, \phi_2 = 1.2$ and $M = 0.5$ for $\eta = 0$.

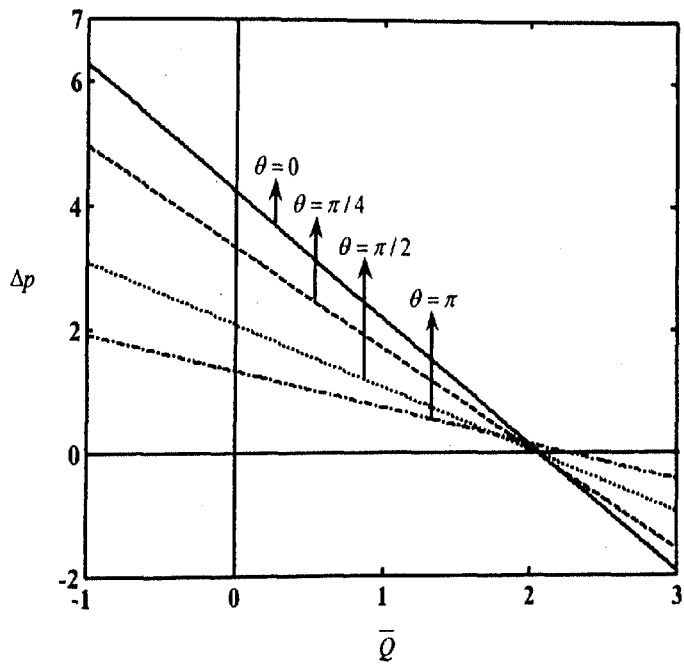

Fig 4.7(ii). The variation of pressure rise Δp with time-averaged volume flow rate $\overline{Q}$ for different phase shifts with $d = 2, \phi_1 = 0.7, \phi_2 = 1.2$ and $M = 0.5$ for $\eta = 1$.

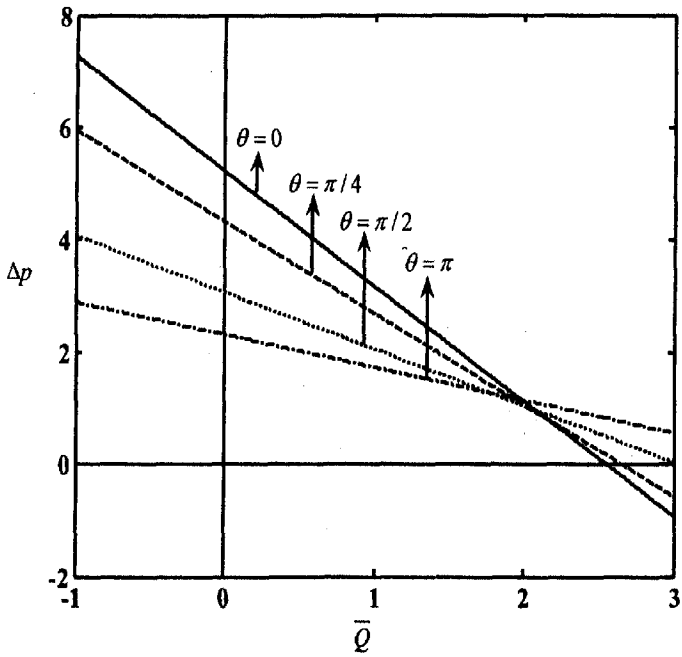

Fig 4.7(iii). The variation of pressure rise Δp with time-averaged volume flow rate $\bar{Q}$ for different phase shifts with $d = 2, \phi_1 = 0.7, \phi_2 = 1.2$ and $M = 0.5$ for $\eta = 2$.